

Structural modulation and physical properties of cobalt-doped layered $La_2M_5As_3O_2$ (M=Cu, Ni) compounds

Lei Yang(杨蕾), Yan-Peng Song(宋艳鹏), Jun-Jie Wang(王俊杰), Xu Chen(陈旭), Hui-Jing Du(杜会静), and Jian-Gang Guo(郭建刚)

Citation: Chin. Phys. B, 2021, 30 (**7**): 076106. DOI: 10.1088/1674-1056/abf349
Journal homepage: http://cpb.iphy.ac.cn; http://iopscience.iop.org/cpb

What follows is a list of articles you may be interested in

Prediction of scandium tetraboride from first-principles calculations: Crystal structures, phase stability, mechanical properties,and hardness

Bin-Hua Chu(初斌华)† and Yuan Zhao(赵元)
Chin. Phys. B, 2021, 30 (**7**): 076107. DOI: 10.1088/1674-1056/abe116

Novel rubidium polyfluorides with F_3, F_4, and F_5 species

Ziyue Lin(林子越), Hongyu Yu(于洪雨), Hao Song(宋昊), Zihan Zhang(张子涵), Tianxiao Liang(梁天笑), Mingyang Du(杜明阳), and Defang Duan(段德芳)
Chin. Phys. B, 2021, 30 (**6**): 066102. DOI: 10.1088/1674-1056/abefc6

Degradation of β-Ga_2O_3 Schottky barrier diode under swift heavy ion irradiation

Wen-Si Ai(艾文思), Jie Liu(刘杰), Qian Feng(冯倩), Peng-Fei Zhai(翟鹏飞), Pei-Pei Hu(胡培培), Jian Zeng(曾健), Sheng-Xia Zhang(张胜霞), Zong-Zhen Li(李宗臻), Li Liu(刘丽), Xiao-Yu Yan(闫晓宇), and You-Mei Sun(孙友梅)
Chin. Phys. B, 2021, 30 (**5**): 056110. DOI: 10.1088/1674-1056/abf107

Ab initio study on crystal structure and phase stability of ZrC_2 under high pressure

Yong-Liang Guo(郭永亮), Jun-Hong Wei(韦俊红), Xiao Liu(刘潇), Xue-Zhi Ke(柯学志), and Zhao-Yong Jiao(焦照勇)
Chin. Phys. B, 2021, 30 (**1**): 016101. DOI: 10.1088/1674-1056/abb3e7

Crystal structure and magnetic properties of disordered alloy $ErGa_{3-x}Mn_x$

Cong Wang(王聪), Yong-Quan Guo(郭永权), Shuo-Wang Yang(杨硕望)
Chin. Phys. B, 2019, 28 (**8**): 086101. DOI: 10.1088/1674-1056/28/8/086101

Structural modulation and physical properties of cobalt-doped layered $La_2M_5As_3O_2$ (M = Cu, Ni) compounds*

Lei Yang(杨蕾)[1,2], Yan-Peng Song(宋艳鹏)[2,3], Jun-Jie Wang(王俊杰)[2,3], Xu Chen(陈旭)[2,3], Hui-Jing Du(杜会静)[1,†], and Jian-Gang Guo(郭建刚)[2,4,‡]

[1] *Key Laboratory for Microstructural Material Physics of Hebei Province, School of Science, Yanshan University, Qinhuangdao* 066004, *China*
[2] *Beijing National Laboratory for Condensed Matter Physics, Institute of Physics, Chinese Academy of Sciences, Beijing* 100190, *China*
[3] *University of Chinese Academy of Sciences, Beijing* 100049, *China*
[4] *Songshan Lake Materials Laboratory, Dongguan* 523808, *China*

(Received 26 February 2021; revised manuscript received 27 March 2021; accepted manuscript online 30 March 2021)

We investigate the structural variation and physical properties of layered $La_2M_5As_3O_2$ (M = Cu, Ni) compound upon Co doping. It is found that the substitution of Co ion just induces the monotonous change of lattice constants without observing the anomalous kink in superconducting $La_2(Cu_{1-x}Ni_x)_5As_3O_2$ solid-solutions. Meanwhile, this doping barely changes As–As bond length in $[M_5As_3]^{2-}$ subunit (±2%), being significantly smaller than 7% shrinkage of that in $La_2(Cu_{1-x}Ni_x)_5As_3O_2$. Therefore, the doping dependence of crystal structure exhibits similar trend with $Ba_{1-x}K_xFe_2As_2$ without the interference of As1–As2 bonding, implying that the Co substitution for Cu/Ni is hole-doped. In terms of physical property, $La_2(Cu_{1-x}Co_x)_5As_3O_2$ turns into itinerant ferromagnetic metal, while $La_2(Ni_{1-x}Co_x)_5As_3O_2$ shows paramagnetism and suppressed structural phase transition upon Co-doping. The distinct structural variation and absence of superconductivity provide important clues to understand the effect of As–As bond in $[M_5As_3]^{2-}$ subunit.

Keywords: crystal structure, As–As covalent bond, transport property

PACS: 61.50.–f, 72.15.–v, 75.20.En, 74.70.Dd **DOI:** 10.1088/1674-1056/abf349

1. Introduction

Discovery of high-temperature superconductivity (SC) of cuprates,[1–3] iron pnictides,[4,5] and iron selenides[6–10] has brought out huge advances in condensed matter physics and material sciences. Typical structure of both iron-based superconductors is a layered form, where the spacer layers are ionic $[La_2O_2]^{2+}$/Ba^{2+}/K^+ and the functional layers are anti-fluorite type $[Fe_2X_2]^{2-}$ (X = P/As or S/Se/Te). The interesting properties like superconducting transition temperature (T_c),[11] quantum critical point,[12] nematic phase,[13] and magnetic fluctuation[14] are intimately determined by the geometry and electron counting of the latter one.

In well-documented reports, chemical doping in the spacer or functional layer can effectively influence the states of $[Fe_2X_2]^{2-}$, T_c, and superconducting property.[15,16] For example, in $ThCr_2Si_2$-type $BaFe_2As_2$, partial replacing divalent Ba^{2+} with monovalent A^+ ions (A = alkali metal) leads to hole-doping superconductors exhibiting dome-like T_c.[5] Alternately, substituting Fe^{2+} with Co^{2+}/Ni^{2+} cation[17,18] or As^{3-} with P^{3-} anion[12] can induce electron-doped superconductors with similar dome-like T_c and many unexpected properties. In terms of crystallography, we can see there are distinct evolutions of crystal structure upon doping. That is, the in-plane lattice a shrinks (expands) and the c-axis expands (shrinks) in hole (electron)-doped $Ba_{1-x}A_xFe_2As_2$,[19–21] which is viewed as competition of intra-layer deformation and interlayer Coulomb attraction due to accumulation of charge in the $[Fe_2X_2]^{2-}$ layers.[22] Once the excess holes are introduced into the $[Fe_2X_2]^{2-}$ layers, the Fe–X bond length and X–Fe–X angle are decreased, leading to an in-plane contraction. Meanwhile, the Coulomb attraction between the positive space layers and negative charged $[Fe_2X_2]^{2-}$ layer weakens, and the expansion of c-axis ensues.

The $Ln_2(Cu_{1-x}Ni_x)_5As_3O_2$ (Ln = La, Pr, Nd) is the first CuAs-based superconductor reported by our group.[23] It possesses a typical layered structure that is consisted of spacer layer $[La_2O_2]^{2+}$ and functional subunit $[M_5As_3]^{2-}$ (M = Cu, Ni, Co) containing strong As–As covalent bond along c-axis.[24,25] For the end-member $Re_2Ni_5As_3O_2$ (Re = La, Ce, Sm),[26] it exhibits a structural phase transition from tetragonal ($I4/mmm$) to orthorhombic (I/mmm) symmetry, and does not change into superconductors at low temperature. The solid-solutions of $Ln_2(Cu_{1-x}Ni_x)_5As_3O_2$ exhibit complex change in structure, where a increases and c decreases as $x < 0.4$, and then a decreases and c increases as $x > 0.4$. At the same time, the As–As bonding length shrinks from 2.81 Å to 2.63 Å, leading to a dome-like T_c with the highest T_c at $x = 0.4$. Since the

*Projected supported by the National Natural Science Foundation of China (Grant Nos. 51922105 and 51772322), the National Key Research and Development Program of China (Grant Nos. 2017YFA0304700 and 2016YFA0300600), and the Beijing Natural Science Foundation, China (Grant No. Z200005).

†Corresponding author. E-mail: hjdu@ysu.edu.cn
‡Corresponding author. E-mail: jgguo@iphy.ac.cn

© 2021 Chinese Physical Society and IOP Publishing Ltd

As–As covalent bond can accumulate or release excess electrons, the empirical rule obtained from $ThCr_2Si_2$-type compounds seems not to be accurate enough to describe the structural change in the layered compounds.

In this work, we prepare two series of solid solutions of $La_2(M_{1-x}Co_x)_5As_3O_2$ (M = Cu, Ni) (x = 0–0.7) and systematically investigate the structural change and physical property. It is found that the As–As bond length only slightly changes (±2%), differing from large shrinkage of that in $La_2(Cu_{1-x}Ni_x)_5As_3O_2$.[23] Meanwhile, we observe that the Co-doping induces monotonous change in a and c unlike the anomalous kink of $La_2(Cu_{1-x}Ni_x)_5As_3O_2$. In addition, $La_2(Cu_{1-x}Co_x)_5As_3O_2$ (x = 0–0.7) exhibits a phase transition from paramagnetism to ferromagnetism as the Co content increases above 0.4. While $La_2(Ni_{1-x}Co_x)_5As_3O_2$ (x = 0–0.7) samples only show paramagnetism, and the structural transition from tetragonal to orthorhombic phase is suppressed. We discuss the structural evolution and the lack of superconductivity from the key aspect of As–As covalent bonding state.

2. Experimental details

Polycrystalline samples of $La_2(M_{1-x}Co_x)_5As_3O_2$ (M = Cu, Ni) (x = 0–0.7) were synthesized by conventional solid-state reactions. The binary precursors LaAs and Cu_3As, NiAs, Co_2As were pre-synthesized by reacting La filings, Cu/Ni/Co powder and As powder at 1000 K for 20 h. Then, the powders of LaAs, Cu_3As, NiAs, Co_2As, La_2O_3, Ni, and Cu were weighted according to the desired ratio, ground, and pelleted under a pressure of 50 MPa in an argon-filled glove box with an O_2 and H_2O content below 1 ppm. The pellet was loaded into an Al_2O_3 crucible, and then sealed into an evacuated silica tube, which was heated at 150 K, hold for 40 h, and then furnace-cooling to room temperature.

Powder x-ray diffraction (PXRD) patterns of the obtained samples were collected using a Panalytical diffractometer with Cu K_α (λ = 1.5408 Å) radiation equipped with a low-temperature cryostat. Rietveld refinement of the PXRD pattern was performed by Fullprof software suites.[27] The electrical resistivity (ρ) was measured through the standard four-wire method in the physical property measurement system (PPMS, Quantum Design). The dc magnetic properties were characterized using a vibrating sample magnetometer (PPMS, Quantum Design).

3. Results and discussion

Figure 1(a) shows the PXRD patterns of the selected $La_2(M_{1-x}Co_x)_5As_3O_2$ (M = Cu, Ni) samples for clarity. There are no obvious impurity peaks in the whole pattern, indicating that the synthesized samples are homogeneous and almost pure phase. All diffraction peaks exhibit monotonous shift with increasing the content of Co. Meanwhile, all the peaks can be indexed with a unit cell of tetragonal symmetry. We determined the crystal structure of pure $La_2Cu_5As_3O_2$ and $La_2Ni_5As_3O_2$ phases and reported them in Refs. [23,26]. Therefore, we can refine the whole PXRD pattern of two series of Co-doped $La_2Cu_5As_3O_2$ and $La_2Ni_5As_3O_2$ samples based on the above structure. The representative profiles are plotted in Fig. 1(b). The refinements of both patterns of $La_2Cu_3Co_2As_3O_2$ and $La_2Ni_3Co_2As_3O_2$ smoothly converge into R_p = 1.92%, R_{wp} = 2.76% and R_p = 1.78% and R_{wp} = 2.43%, respectively. Here we think that the Cu/Ni atoms are random substituted by the Co ions without changing the structural symmetry. Meanwhile, the Co substitution of Cu (Ni) is more likely to be hole-doping due to two (one) fewer 3d electrons according to the results in literatures.[28,29]

The crystal structure of $La_2M_5As_3O_2$ (M = Cu, Ni, Co) is drawn in Fig. 2(a). It can be seen that functional $[M_5As_3]^{2-}$ subunit and fluorite-type $[La_2O_2]^{2+}$ layers are alternately stacked along the c-axis. In a $[Cu_5As_3]^{2-}$ subunit, the $M1$ atoms are separated by a central $M2$ plane and the As1–As2 are connected by the covalent bond with length of 2.81 Å. The bonding details are shown in Fig. 2(b). The Co-content dependent unit cell parameters are summarized and plotted in Figs. 2(c) and 2(d). The data of $La_2(Cu_{1-x}Ni_x)_5As_3O_2$ are taken from Ref. [23] and shown as green square. We firstly examine the crystallographic parameters of $La_2(Ni_{1-x}Co_x)_5As_3O_2$ in the right panels of Figs. 2(c) and 2(d). As x below the doping limit of 0.7, it is found that the lattice constant a continuously decreases from 4.0691 Å to 4.0162 Å, however, the c inversely increases from 22.482 Å to 22.972 Å. The obtained c/a ratio linearly increases from 5.54 to 5.72, which perfectly falls into the extrapolated line of $La_2(Cu_{1-x}Ni_x)_5As_3O_2$. It again confirms the validation of the present experimental data. For the volume of a unit cell, it just slightly decreases from 372 Å^3 to 370 Å^3. For the $La_2(Cu_{1-x}Co_x)_5As_3O_2$, the a monotonously decreases from 4.1404 Å to 4.0621 Å, differing from that of $La_2(Cu_{1-x}Ni_x)_5As_3O_2$. While its c-axis firstly keeps a constant and gradually saturates to be 23.0 Å. The c/a ratio slightly increases from 5.54 to 5.66 and the volume linearly decreases from 391 Å^3 to 379 Å^3. The shrinkage of a and expansion of c indicate that the Co-substitution is like hole-doping as suggested in hole-doped layered compounds of $Ba_{1-x}K_xFe_2As_2$[19] and $Ba_{1-x}Na_xFe_2As_2$.[20] In addition, the variations of lattice constants of two Co-doped cases are significantly different from those of $La_2(Cu_{1-x}Ni_x)_5As_3O_2$, in which the a, c, and c/a ratio show non-monotonous changes and the highest T_c perfectly occurs at the structural anomaly of x_{Ni} = 0.4.

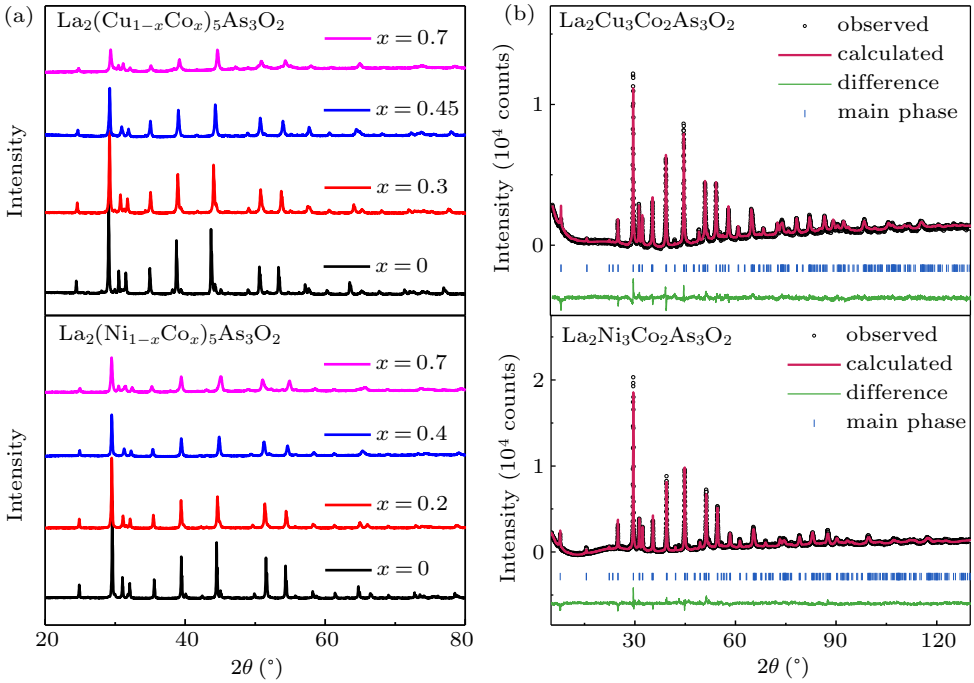


Fig. 1. (a) Powder XRD patterns of typical $La_2(M_{1-x}Co_x)_5As_3O_2$ (M = Cu, Ni) samples. (b) Rietveld refinement profiles of two representative samples of $La_2Cu_3Co_2As_3O_2$ and $La_2Ni_3Co_2As_3O_2$.

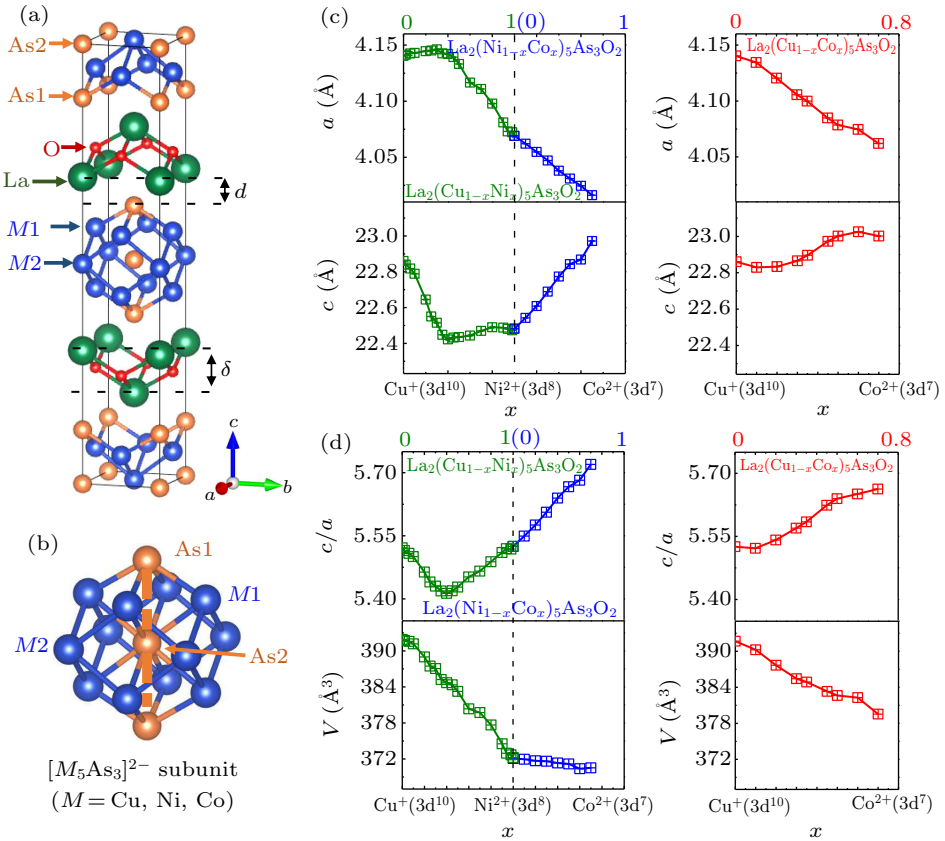


Fig. 2. (a) Crystal structure of $La_2(M_{1-x}Co_x)_5As_3O_2$ (M = Cu, Ni, Co). (b) Structure of $[M_5As_3]^{2-}$ subunit. (c) Lattice parameters a, c, c/a and volume of unit cell V of three series of samples. The data of $La_2(Cu_{1-x}Ni_x)_5As_3O_2$ are taken from Ref. [23]. The error bars are within the hollow squares.

In order to analyze the details of structural evolution, we first check the change in interlayer spacing (d) between $[La_2O_2]^{2+}$ layer and $[M_5As_3]^{2-}$ upon Co doping. It is found that d linearly increases within the limit of experimental error in Fig. 3(a). The increments of d are 0.06 Å and 0.13 Å for $La_2(Ni_{1-x}Co_x)_5As_3O_2$ and $La_2(Cu_{1-x}Co_x)_5As_3O_2$, respectively. At the same time, in Fig. 3(b), the thickness (δ) of $[La_2O_2]^{2+}$ layers also increases, which can partially account for the trend of increase in c-axis. For the $[M_5As_3]^{2-}$, the thickness equals to two times of As1–As2 bond length. In

Fig. 3(c), we plot the variation of As1–As2 bond lengths of three systems. In Ni-doped $La_2Cu_5As_3O_2$, the length almost linearly decreases from 2.81 Å to 2.63 Å with a kink at $x = 0.4$. However, as further lowering the number of d electrons from $3d^8$ (Ni^{2+}) to $3d^7$ (Co^{2+}), the As1–As2 bond length inversely increases slightly and then keeps a constant of 2.66 Å. For Co-doped $La_2Cu_5As_3O_2$, the As1–As2 bond length slightly decreases from 2.81 Å to 2.73Å accompanying a tiny kink at $x = 0.5$, see Fig. 3(d). From the above results, one can see that the expansion of c-axis mainly comes from the increment of interlayer spacing d and thickness δ of $[La_2O_2]^{2+}$ layer because the thickness of $[M_5As_3]^{2-}$ changes little.

Figure 4 shows temperature-dependent transport property of $La_2(Cu_{1-x}Co_x)_5As_3O_2$ (x = 0–0.7) from 2–300 K. As shown in the temperature-dependent resistivity $\rho(T)$ of Fig. 4(a), all samples with different Co contents show metallic conductivity in the measured temperature range. As we know, the parent compound $La_2Cu_5As_3O_2$ is a superconductor with $T_c = 0.65$ K. There is a jump at 80 K in $\rho(T)$ curve, implying a density-wave phase transition. It is found that with the increase of Co ion, the resistivity kink disappears for all of the doped samples. Meanwhile, the magnitude of magnetic susceptibility (χ) gradually increases with increasing Co content, as shown in Fig. 4(b). In the inset, the χ of the sample with a low concentration of Co is smaller than 4×10^{-3} emu/mol·Oe, and the temperature-dependent χ shows typical Curie–Weiss behavior, suggesting that there are enhanced magnetic interactions between Co ions.[30] As $x > 0.4$, the $\chi(T)$ curves exhibit typical ferromagnetic phase transitions with Curie temperature around 120 K and the maximal χ of $x = 0.4$ sample is 0.38 emu/mol·Oe. Figure 4(c) shows the temperature dependence of $\chi(T)$ per mol Co of three samples measured under a magnetic field $H = 1$ T. The inset shows three $1/\chi(T)$ curves and the data between 120 K and 250 K can be well fitted by the Curie–Weiss equation $\chi = C/(T - \theta)$, where θ is the Curie temperature that is related to the effective interaction between the magnetic moments. C is the Curie constant contributed by the effective magnetic moment. The obtained θ are 101.4 K, 99.1 K, and 66.9 K for $x = 0.4$, 0.45, and 0.6, respectively, and the positive values indicate that the magnetic interactions are ferromagnetic. We calculate the effective magnetic moment through $\mu_{\text{eff}} = \sqrt{8C/n}$, where n is the number of magnetic atoms. The effective magnetic moments (μ_{eff}) per Co ion are 1.47 μ_B, 1.74 μ_B, and 1.41 μ_B, which are close to the classic value (1.73 μ_B) of low-spin state of Co^{2+} ion. Figure 4(d) shows the H-dependent magnetization (M) loops of $La_2Cu_{2.75}Co_{2.25}As_3O_2$ measured at different temperatures. As $T > 200$ K, the M–H curves linearly increase and exhibit paramagnetic characters. As $T < 100$ K, the M gradually increases to a constant value with increasing H. Meanwhile, the saturation magnetic moment μ_s gradually increases as the temperature decreases. At $T = 10$ K, the saturated magnetic moment μ_s of $La_2Cu_{2.75}Co_{2.25}As_3O_2$ is 0.29 μ_B. But the M–H curves do not show large hysteresis in low field range, and the coercive force is 50 Oe, which can be viewed as a typical soft magnet. Meanwhile, since the μ_s is much smaller than μ_{eff} and the sample is metallic, the $La_2(Cu_{1-x}Co_x)_5As_3O_2$ is an itinerate ferromagnet.

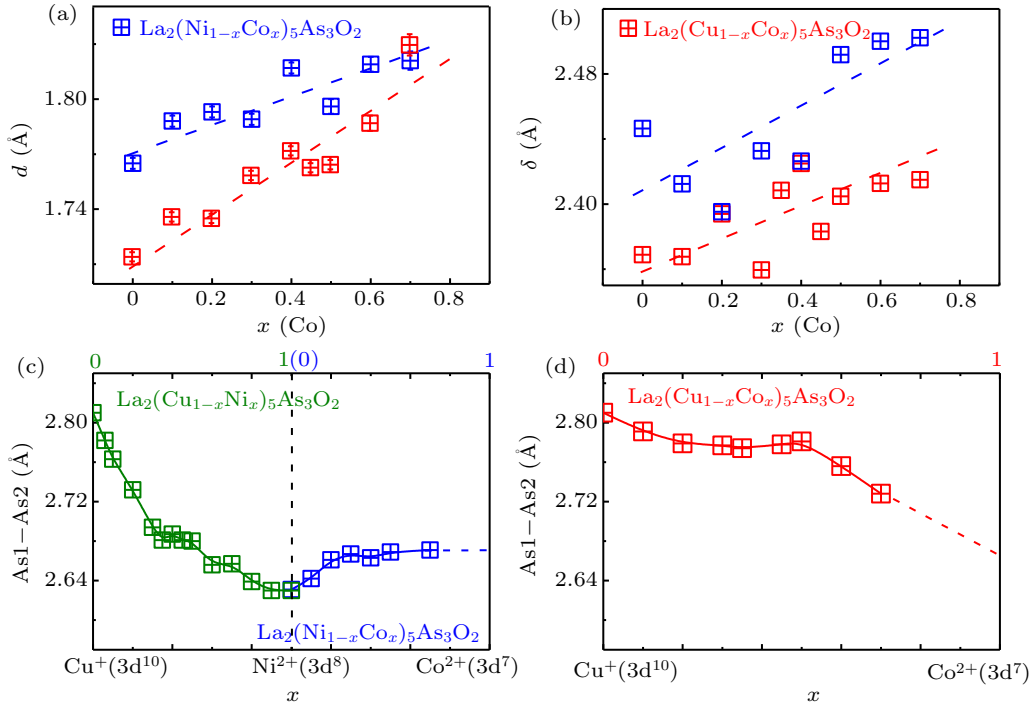


Fig. 3. (a) and (b) Co-content dependent interlayer spacing d between $[La_2O_2]^{2+}$ layer and $[M_5As_3]^{2-}$ subunit, and thickness (δ) of $[La_2O_2]^{2+}$ layer. Dashed lines are guided to eyes. (c) and (d) As1–As2 bond lengths in three series of samples. The data of $La_2(Cu_{1-x}Ni_x)_5As_3O_2$ are taken from Ref. [23].

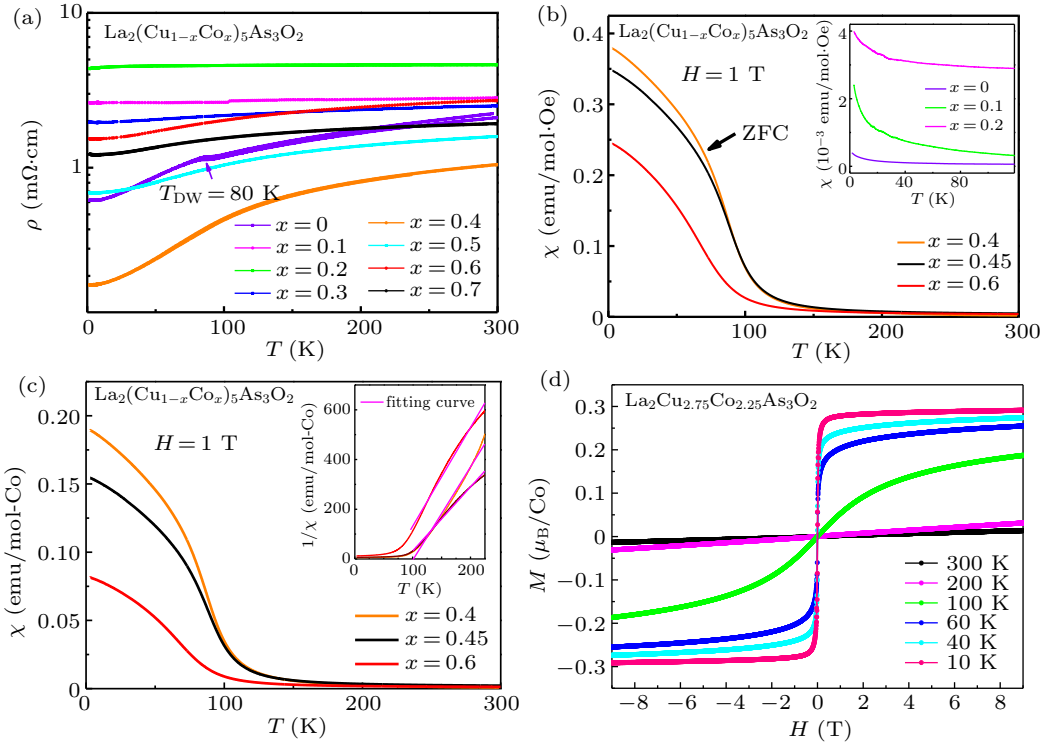


Fig. 4. Physical properties of $La_2(Cu_{1-x}Co_x)_5As_3O_2$. (a) Temperature-dependent electrical resistivity of $La_2(Cu_{1-x}Co_x)_5As_3O_2$ ($x = 0$–0.7) from 2 K–300 K. (b) Temperature-dependent magnetic susceptibility (χ) measured at $H = 1$ T. Inset shows the $\chi(T)$ curves of $x = 0$, 0.1, and 0.2 samples. (c) $\chi(T)$ curves for per mol Co ion. Inset shows their inverse curves. Pinks lines are fitting curves as shown in the main text. (d) M–H loops of different temperatures.

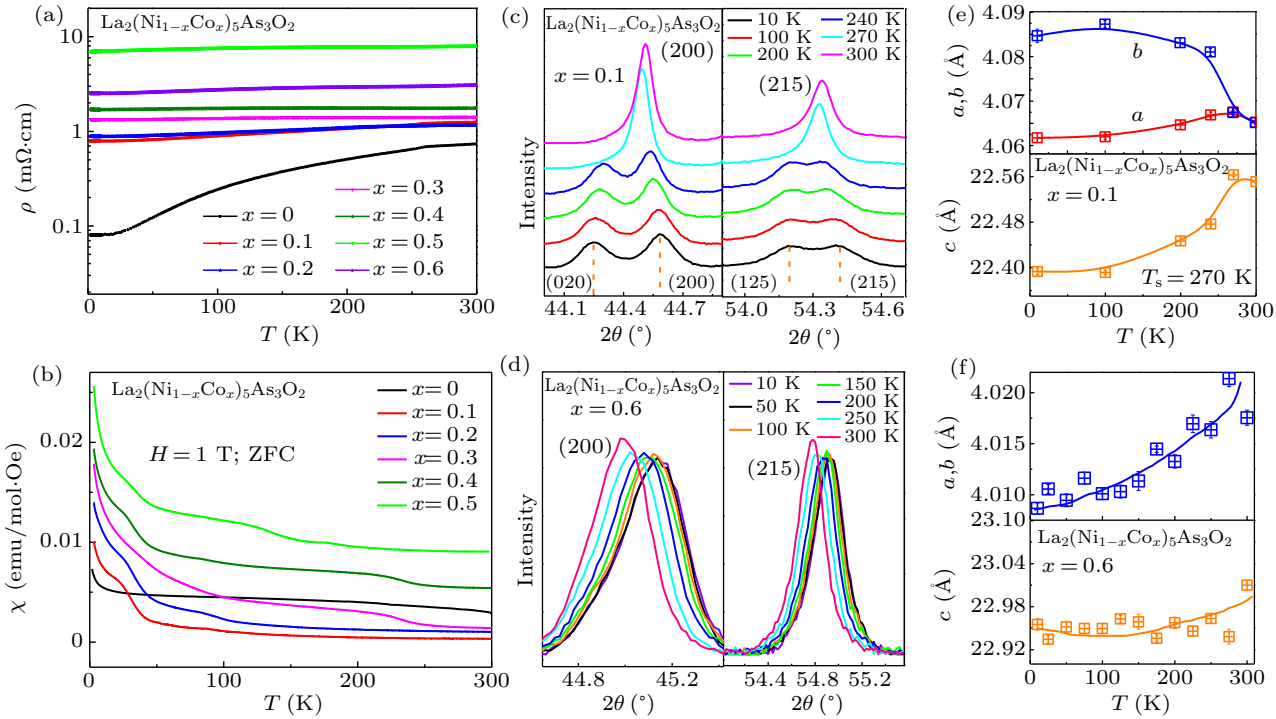


Fig. 5. Physical property and structural phase transition of $La_2(Ni_{1-x}Co_x)_5As_3O_2$. (a)–(b) Temperature-dependent electrical resistivity (ρ) and magnetic susceptibility (χ) measured at $H = 1$ T. (c)–(d) (200) and (215) diffraction peaks of $x = 0.1$ and $x = 0.6$ samples measured from 10 K–300 K. (e)–(f) Temperature-dependent lattice constants of $La_2(Ni_{1-x}Co_x)_5As_3O_2$ ($x = 0.1$ and 0.6). For $x = 0.1$, there is a phase transition evidenced by splitting of a-lattice parameters below 270 K.

Now we turn to investigate the transport property of $La_2(Ni_{1-x}Co_x)_5As_3O_2$ ($x = 0$–0.7). Figure 5(a) shows the $\rho(T)$ curves of all samples. It can be seen that all samples behave as a metal in the measured temperature range, and the ρ of the doped samples has increased by 1–2 orders of magnitude due to magnetic or disorder scattering. Another reason is that the As1–As2 covalent bond status changes the carrier concentration, and the synergistic effect enhances the resis-

tivity. Figure 5(b) shows the magnetic susceptibility $\chi(T)$ of $La_2(Ni_{1-x}Co_x)_5As_3O_2$ ($x = 0$–0.7) with $H = 1$ T. We can see that the $\chi(T)$ curves of all samples show paramagnetic behavior in the measured range. Meanwhile, with increasing the Co content, $\chi(T)$ gradually increases, the value is between 0.007 emu/mol·Oe and 0.025 emu/mol·Oe. Compared with the $\chi(T)$ of $La_2(Cu_{1-x}Co_x)_5As_3O_2$, the high concentration of Co does not induce ferromagnetic phase transitions.

Since $La_2Ni_5As_3O_2$ undergoes a structural phase transition from tetragonal ($I4/mmm$) to orthorhombic (I/mmm) symmetry at 270 K, we measured the PXRD pattern of $La_2(Ni_{1-x}Co_x)_5As_3O_2$ ($x = 0.1$ and 0.6) from 300 K to 10 K so as to check the structural evolution upon Co doping. Figure 5(c) shows the temperature-dependent (200) and (215) diffraction peaks of $x = 0.1$ sample. We can see that the peaks (200) and (215) split into (200)/(020) and (125)/(215), respectively, as the temperature is lower than 270 K. It means that the sample undergoes a similar structural phase transition like $La_2Ni_5As_3O_2$. In Fig. 5(d), it can be seen that the (200) and (215) diffraction peaks of $x = 0.6$ sample shift towards higher angle without splitting with decreasing temperature, indicating that the phase transition has been suppressed. We use the orthogonal space group I/mmm (No. 71) to index the PXRD pattern at 10 K. The lattice constants are $a_0 = 4.0616(2)$ Å, $b_0 = 4.0847(8)$ Å, and $c_0 = 22.393(3)$ Å. Figure 5(e) shows the temperature dependence of the lattice constants of $x = 0.1$ sample, where a_0 and c_0 gradually decrease, and b_0 gradually increases and becomes saturated as T decreases. For $x = 0.6$ sample, the lattice constants a and c just monotonously shrink during cooling, see Fig. 5(f).

Let us briefly discuss the structural variation and physical property of $La_2M_5As_3O_2$ (M = Cu, Ni) under Co doping. As previously reported doping behaviors in $BaFe_2As_2$, the substitution of Fe by Co/Ni/Cu with more 3d electrons leads to electron-type doping and the doping-dependent superconductivity can be scaled by the net carrier concentrations.[31] In the present work, the substitution of Co ($3d^7$) into $La_2M_5As_3O_2$ (M = Cu, Ni) should be hole-doped type, which is evidenced by the expansion of ab-plane and the shrinkage of c-axis above. In $La_2Cu_5As_3O_2$, the Ni-doping can induce a dome-like T_c; while the Co-doping only kills the DW-like transition and then induces ferromagnetic phase transitions ~ 100 K rather than superconductivity. Furthermore, we found that the Co^{2+} ions may exhibit unusual low-spin state ($S = 1/2$) under this unique coordination. However, since the scattering lengths of Co^{2+} and Cu^{+} for x-ray are pretty close, we cannot unambiguously identify which site the Co^{2+} ions preferentially occupy. For $La_2(Ni_{1-x}Co_x)_5As_3O_2$, the Co-doping increases the As–As bond length a little bit from 2.63 Å to 2.66 Å, however, the increment is too small. It does not reach the As1–As2 bond length of $La_2(Cu_{1-x}Ni_x)_5As_3O_2$ superconductor. Hence, the Co-doping does not induce superconductivity in the present work.

It is known that the Co-doping should not follow the rigid band model like the case of Co/Ni/Cu-doped $BaFe_2As_2$,[31,32] where partial induced electrons are localized around the dopant sites and do not contribute to the conductivity. Given the complex structural change like 40% kink in $La_2(Cu_{1-x}Ni_x)_5As_3O_2$ and anisotropic change in thickness of $[La_2O_2]^{2+}$ layer and $[M_5As_3]^{2-}$ subunit, it is hard to reconcile the lattice variation with the simple electron counting. The dependence of physical properties on Co/Ni doping in $Ln_2Cu_5As_3O_2$ (Ln = La, Pr, Nd) should be more complicated due to the variation of As–As covalent bonding status. Detailed structural analyses and low-temperature measurements are needed to clarify the above two issues.

4. Conclusion

We have investigated the structure and low-temperature property of $La_2(M_{1-x}Co_x)_5As_3O_2$ (M = Cu, Ni; $x = 0$–0.7). It is found that the doped Co ions induce simpler structural variation than those of $La_2(Cu_{1-x}Ni_x)_5As_3O_2$ because the As–As bonding status barely changes. Furthermore, the Co-doping induces a paramagnetic to ferromagnetic phase transition as $x > 0.4$ in $La_2(Cu_{1-x}Co_x)_5As_3O_2$ and suppresses the structural phase transition at $x = 0.6$ in $La_2(Ni_{1-x}Co_x)_5As_3O_2$. Unfortunately, all the doped samples are non-superconductive in the temperature range of 2–300 K. From the view of As–As bond, it demonstrates that the bonding states could determine the crystal evolutions and influence the transport property.

References

[1] Bednorz J G and Mueller K 1986 *Z. Phys. B* **64** 189
[2] Yang C, Liu Y, Wang Y, Feng L, He Q, Sun J, Tang Y, Wu C C, Xiong J, Zhang W L, Lin X, Yao H, Liu H W, Fernandes G, Xu J, Valles J, Wang J and Li Y R 2019 *Science* **366** 1505
[3] Ai P, Gao Q, Liu J, Zhang Y X, Li C, Huang J W, Song C Y, Yan H T, Zhao L, Liu G D, Gu G D, Zhang F F, Yang F, Peng Q J, Xu Z Y and Zhou X J 2019 *Chin. Phys. Lett.* **36** 067402
[4] Kamihara Y, Watanabe T, Hirano M and Hosono H 2008 *J. Am.Chem. Soc.* **130** 3296
[5] Rotter M, Tegel M and Johrend D 2008 *Phys. Rev. Lett.* **101** 107006
[6] Hsu F C, Luo J Y, Yeh K W, Chen T K, Huang T W, Wu P M, Lee Y C, Huang Y L, Chu Y Y, Yan D C and Wu M K 2008 *Proc. Natl. Acad. Sci. USA* **105** 14262
[7] Guo J G, Jin S F, Wang G, Wang S C, Zhu K X, Zhou T T, He M and Chen X L 2010 *Phys. Rev. B* **82** 180520
[8] Lai X F, Zhang H, Wang Y Q, Wang X, Zhang X, Lin J H and Huang F Q 2015 *J. Am. Chem. Soc.* **137** 10148
[9] Wang C W, Wang M X, Jiang J, Yang H F, Yang L X, Shi W J, Lai X F, Mo S K, Barinov A, Yan B H, Liu Z, Huang F Q, Jia J F, Liu Z K and Chen Y L 2020 *Chin. Phys. B* **29** 047401
[10] Zhang S Y, Miao G Y, Guan J Q, Xu X F, Liu B, Yang F, Wang W H, Zhu X T and Guo J D 2019 *Chin. Phys. Lett.* **36** 107404
[11] Ren Z A, Lu W, Yang J, Yi W, X. Shen X L, Li Z C, Che G C, Dong X L, Sun L L, Zhou F and Zhao Z X 2008 *Chin. Phys. Lett.* **25** 2215
[12] Kasahara S, Shibauchi T, Hashimoto K, Ikada K, Tonegawa S, Okazaki R, Shishido H, Ikeda H, Takeya H, Hirata K, Terashima T and Matsuda Y 2010 *Phys. Rev. B* **81** 184519

[13] Dai P C, Hu J P and Dagotto E 2012 *Nat. Phys.* **8** 709

[14] Chu J H, Analytis J G, Greve K D, McMahon P L, Islam Z, Yamamoto Y and Fisher I R 2010 *Science* **329** 824

[15] Sun R J, Jin S F, Deng J, Hao M N, Zhao L L, Fan X, Sun X N, Guo J G and Gu L 2019 *Chin. Phys. B* **28** 067401

[16] Ni S L, Hu W, Shen P P, Wei Z X, Liu S B, Li D, Yuan, J, Yu L, Jin K, Zhou F, Dong X L and Zhao Z X 2019 *Chin. Phys. B* **28** 127401

[17] Ni N, Tillman M E, Yan J Q, Kracher A, Hannahs S T, Bud'ko S L and Canfield P C 2008 *Phys. Rev. B* **78** 214515

[18] Canfield P C, Bud'ko S L, Ni Ni, Yan J Q and Kracher A 2009 *Phys. Rev. B* **80** 060501

[19] Chen H, Ren Y, Qiu Y, Bao W, Liu R H, Wu G, Wu T, Xie Y L, Wang X F, Huang Q and Chen X H 2009 *Euorphys. Lett.* **85** 17006

[20] Wang L, Hardy F, Böhmer A E, Wolf T, Schweiss P and Meingast C 2016 *Phys. Rev. B* **93** 014514

[21] Ni N, Thaler A, Yan J Q, Kracher A, Colombier E, Bud'ko S L, Canfield P C and Hannahs S T 2010 *Phys. Rev. B* **82** 024519

[22] Liu Y, Wang G, Ying T, Lai X, Jin S, Liu N, Hu J and Chen X 2016 *Advanced Science* **3** 1600098

[23] Chen X, Guo J G, Gong C S, Cheng E J, Le C C, Liu N, Ying T P, Zhang Q H, Hu J P, Li S Y and Chen X L 2019 *Science* **14** 171

[24] Yakita H, Ogino H, Okada T, Yamamoto A, Kishio K, Tohei T, Ikuhara Y, Gotoh Y, Fujihisa H, Kataoka K, Eisaki H and Shimoyama J I 2014 *J. Am. Chem. Soc.* **136** 846

[25] Jia S, Jiramongkolchai P, Suchomel M R, Toby B H, Checkelsky J G, Ong N P and Cava R J 2011 *Nat. Phys.* **7** 207

[26] Chen X, Guo J G, Gong C S, Cheng E J, Song Y P, Ying T P, Deng J, Li S Y and Chen X L 2019 *Inorganic Chemistry* **58** 2770

[27] Rodríguez-Carvajal J 1993 *Physica B* **192** 55

[28] Rotter M, Pangerl M, Tegel M and Johrendt D 2008 *Cheminform* **47** 7949

[29] Sefat A S, Jin R, Mcguire M A, Sales B C, Singh D J and Mandrus D 2008 *Phys. Rev. Lett.* **101** 117004

[30] Shen S J, Wang G, Jin S F, Huang Q Z, Ying T P, Li D D, Lai X F, Zhou T T, Zhang H, Lin Z P, Wu X Z and Cen X L 2014 *Chem. Mater.* **26** 6221

[31] Ideta S, Yoshida T, Nishi I, Fujimori A, Kotani Y, Ono K, Nakashima Y, Yamaichi S, Sasagawa T, Nakajima M, Kihou K, Tomioka Y, Lee C H, Iyo A, Eisaki H, Ito T, Uchida S and Arita R 2013 *Phys. Rev. Lett.* **110** 107007

[32] Kim M G, Lamsal J, Heitmann T W, Tucker G S, Pratt D K, Khan S N, Lee Y B, Alam A, Thaler A, Ni N, Ran S, Bud'ko S L, Marty K J, Lumsden M D, Canfield P C, Harmon B N, Johnson D D, Kreyssig A, McQueeney R J, and Goldmanet A I 2012 *Phys. Rev. Lett.* **109** 167003